The Active Site of the Bacterial Nitric Oxide Reductase Is a Dinuclear Iron Center†

Janneke Hendriks,‡ Antony Warne,‡ Ulrich Gohlke,‡ Tuomas Haltia,§ Claudia Ludovici,|| Mathias Lübben,|| and Matti Saraste*,‡

European Molecular Biology Laboratory, Meyerhofstrasse 1, Postfach 102209, D-69012 Heidelberg, Germany, Department of Medical Chemistry, Institute of Biomedical Sciences, University of Helsinki, P.O. Box 8, FIN-00014 Helsinki, Finland, and Department of Biophysics, University of Bochum, Universitätsstrasse 150, D-44780 Bochum, Germany

Received April 27, 1998; Revised Manuscript Received July 7, 1998

ABSTRACT: A novel, improved method for purification of nitric oxide reductase (NOR) from membranes of *Paracoccus denitrificans* has been developed. The purified enzyme is a cytochrome *bc* complex which, according to protein chemical and hydrodynamic data, contains two subunits in a 1:1 stoichiometry. The purified NorBC complex binds 0.87 g of dodecyl maltoside/g of protein and forms a dimer in solution. Similarly, it is dimeric in two-dimensional crystals. Images of these crystals have been processed at 8 Å resolution in projection to the membrane. The NorB subunit is homologous to the main catalytic subunit of cytochrome oxidase and is predicted to contain the active bimetallic center in which two NO molecules are turned over to N_2O. Metal analysis and heme composition implies that it binds two B-type hemes and a nonheme iron but no copper. NorC is a membrane-anchored cytochrome *c*. Fourier transform infrared spectroscopy shows that carbon monoxide dissociates from the reduced heme in light and associates with another metal center which is distinct from the copper site of heme/copper oxidases. Electron paramagnetic resonance spectroscopy reveals that NO binds to the reduced enzyme under turnover conditions giving rise to signals near $g = 2$ and $g = 4$. The former represents a typical nitrosyl-ferroheme signal whereas the latter is a fingerprint of a nonheme iron/NO adduct. We conclude that the active site of NOR is a dinuclear iron center.

Denitrification is employed by several soil and marine bacteria as an alternative to the respiratory activity with dioxygen (*1*, *2*). It constitutes an important part of the nitrogen cycle, reversing nitrogen fixation and reforming free nitrogen gas. The enzyme that forms the N−N bond during denitrification is nitric oxide reductase. NOR[1] is a membrane-bound cytochrome *bc* complex which catalyses the reduction of two NO molecules into N_2O and water with concomitant consumption of two protons and two electrons donated by cytochrome *c* (*2*−*4*). As isolated, the enzyme comprises two subunits, but genetic evidence suggests the presence of additional subunits in situ which may be lost during purification (*5*).

The smaller subunit (NorC) is a membrane-bound cytochrome *c* and probably the electron entry site of the enzyme. The larger subunit (NorB) is predicted to contain 12 transmembrane helices and to bind two protohemes. It is also thought to contain a nonheme iron center, which together with one of the *b*-type hemes is believed to assemble the active site where NO is reduced (*3*). NorB is homologous to the largest subunit of heme-copper cytochrome oxidases (COX1, see refs *6*−*9*). COX1 binds a 6-coordinated low-spin heme and a 5-coordinated high-spin heme, and the latter forms the active site with a copper atom (Cu_B) (*10*, *11*). The sequence of NorB contains all six invariant histidines which are the ligands of the low- and high-spin hemes and Cu_B in COX1, in topologically correct positions of the predicted membrane-spanning helices.

Despite its homology with the heme-copper oxidases, NOR does not contain copper. Only iron has been found in the NOR preparations until now, and the total amount of Fe typically exceeds that accounted for by the hemes (*12*−*14*). Consequently, it has been proposed that the active site of NOR is composed of a magnetically coupled pair of a heme and a nonheme iron and that the nonheme iron occupies the position of Cu_B in cytochrome oxidase. This further suggests that the nonheme iron is coordinated to the same three histidine side chains as Cu_B in COX1. It has been noticed that the *Paracoccus* NOR can also reduce oxygen (*15*, *16*).

A recent spectroscopic study (*17*) supports the presence of a spin-coupled di-iron center in NOR, but direct evidence for an iron−iron dinuclear site in NOR is missing. In this report, we have studied the nature of the active site in NOR by allowing the enzyme to react with its paramagnetic substrate NO and by monitoring the reaction with EPR

† T.H. has received financial support from the Academy of Finland and the Sigrid Juselius Foundation. We gratefully acknowledged the support of Klaus Gerwert (Bochum, Germany) with FTIR measurements; these were supported by the Deutsche Forschungsgemeinschaft (SFB 394-C6 to M.L.).

* Corresponding author. Tel: 49-6221-387365. Fax: 49-6221-387306. E-mail: saraste@embl-heidelberg.de.

‡ European Molecular Biology Laboratory.

§ University of Helsinki.

|| University of Bochum.

[1] Abbreviations: AEBSF, 4-(2-aminoethyl)-benzolsulphonylfluoride; DM, *n*-dodecyl β-D-maltoside; EPR, electron paramagnetic resonance; FTIR, Fourier transform infrared spectroscopy; IMAC, immobilised-metal-ion affinity chromatography; NOR, nitric oxide reductase; QSHP, Q-Sepharose high performance; SDS−PAGE, polyacrylamide gel electrophoresis in the presence of sodium dodecyl sulphate; TMPD, *N*,*N*,*N*′,*N*′-tetramethyl-*p*-phenylenediamine; TXRF, total reflection X-ray fluorescence.

S0006-2960(98)00943-X CCC: $15.00
Published on Web 09/02/1998

spectroscopy. The EPR data suggest that a high-spin nonheme iron constitutes part of the active site and, as expected, there is no copper in the active site. The latter is confirmed by CO-binding experiments using FTIR spectroscopy and supported by metal analysis of an improved NOR preparation, which is not contaminated with other metalloproteins. This preparation is also the basis of further structural studies on NOR. Here, we report the first results of the image processing of electron micrographs of two-dimensional NOR crystals.

MATERIALS AND METHODS

Bacterial Growth and Preparation of Membranes. The *Paracoccus denitrificans* strain PD27.21 (Δcbb_3) (*18*), which lacks the cbb_3-type cytochrome oxidase and carries a kanamycin resistance gene, was used in this study. A 0.5 L preculture was grown aerobically at 30 °C in Luria-Bertani medium containing 25 mg/mL kanamycin to the optical density of 0.5 at 600 nm and used for the inoculation of a 125 L fermentor. Growth was continued in the fermentor without aeration at 35 °C in a minimal medium containing 50 mM sodium succinate and 100 mM potassium nitrate at the initial pH 7 (see ref *19*). After growth for 20 h, the production of gas was observed in the fermentor, the cells were harvested by ultrafiltration and centrifugation, and washed with 20 mM Tris-HCl buffer, pH 8.0, before storage at −80 °C. The average yield was 250 g of wet cells. For membrane preparation, 125 g of thawed cells was processed as described previously (*20*), except that 0.2 mM 4-(2-aminoethyl)-benzol-sulfonyl fluoride (AEBSF) was used throughout as a protease inhibitor in preference to phenylmethyl sulfonyl fluoride.

Solubilization of Membranes and Protein Purification. Protein purification was carried out using a Pharmacia P-50 Gradifrac System operated at 6 °C with self-packed columns. All column-packing materials were obtained from Pharmacia. Column chromatography was monitored at 280 nm. Sample loading was carried out directly through the pump. For the preparation of samples used in spectroscopic studies and activity assays, all buffers were thoroughly degassed and sparged with nitrogen, and fractions were collected under nitrogen.

For solubilization, thawed membranes (600−800 mg of protein) were suspended to 250 mL of 20 mM Tris-HCl containing NaCl (50 mM), EDTA (1 mM), AEBSF (0.5 mM), and *n*-dodecyl β-D-maltoside (DM, 2.0 g/g protein) and centrifuged at 200000*g* for 1 h at 4 °C. The supernatant was applied to a preequilibrated 175 mL (5 cm diameter) Q-Sepharose high performance (QSHP) column. Buffers used for anion exchange were (A) 20 mM Tris-HCl, pH 7.6, 0.1 mM EDTA, and 0.02% DM and (B) 20 mM Tris-HCl, pH 7.6, 1 M NaCl, and 0.02% DM (protease inhibitors were not used after membrane solubilization). In the first chromatography step, EDTA was only added to buffer A to avoid interference with the second step which employed immobilized metal-ion affinity chromatography (IMAC). An initial gradient of 0−20% buffer B (100 mL) was followed by a gradient of 20−50% buffer B (1200 mL). The column was run at 20 mL/min. Fractions containing NOR eluted approximately at 0.4 M NaCl. These were directly loaded onto a 40 mL (2.6 cm diameter) chelating Sepharose fast flow column loaded with Cu^{2+} according to the manufacturer's instructions and preequilibrated with the IMAC buffer A (20 mM Tris-HCl, pH 7.6, 0.5 M NaCl, 0.1 mM imidazole, and 0.02% DM). The IMAC buffer B was the same as A but, in addition, contained 50 mM imidazole. After loading of the sample, a gradient of 0 to 5% buffer B (250 mL) was applied. The imidazole concentration was maintained for a further 500 mL of the eluent before the application of a second gradient of 5 to 100% buffer B (50 mL) with which NOR was eluted. Sample application and elution were carried out at 10 mL/min.

The fractions containing NOR were diluted 3-fold with the anion-exchange buffer A and applied to a 20 mL (1.6 cm diameter) QSHP column which had been preequilibrated with the same buffer. For this second QSHP column, both buffers A and B contained 0.5 mM EDTA. After sample loading, an initial 0 to 20% gradient of buffer B (20 mL) was applied; this was followed by a 20 to 50% gradient of buffer B (200 mL). Sample application and elution was carried out at 4 mL/min. The purified NOR eluted at 0.4 M NaCl and was concentrated by ultrafiltration with a 50 kDa cutoff membrane, either in a stirred cell if concentration under nitrogen gas was required or with centrifuge concentrators. Purified protein was frozen in liquid nitrogen at a concentration of 4−20 mg/mL.

Gel filtration was carried out at room temperature with a Pharmacia FPLC and linked Superose 6 and 12 HR10/30 columns for further polishing, determination of detergent binding or estimation of molecular weight. The columns were preequilibrated with 20 mM Tris-HCl, 0.5 mM EDTA, 50 mM NaCl, and 0.02% DM. The flow rate was 0.35 mL/min. The sample size was restricted to 100 mL with a protein concentration of 5−10 mg/mL. For the estimation of molecular weight, the columns were calibrated with the soluble protein standards ferritin, thyroglobulin, catalase, and aldolase in the absence of detergent.

Protein, Heme, and Metal Determinations. The BCA method (Pierce) was used with the bovine serum albumin as a standard for the estimation of protein concentrations of membrane preparations and partially purified NOR samples. For the purified enzyme, the protein concentration was determined using the molar absorptivity 180 mM^{-1} cm^{-1} at 280 nm for the denatured protein (*21*). This value was calculated from the aromatic amino acid composition for the 1:1 NorB/NorC complex as given by the sequence data (*5*).

Heme was quantified by recording pyridine hemochrome spectra as described previously (*20*) and using the inverse matrix method for simultaneous determination of hemes A, B, and C (*22*). Iron and copper content was analyzed with flameless atomic absorption and colorimetry using ferrozine by Limbach and Partner (Heidelberg, Germany) and related to the protein measured as above. Metal analysis by total reflection X-ray fluorescence [TXRF (*23*)] was performed at the Institute of Inorganic Chemistry, University of Frankfurt; these data are related to the sulfur content (31 S/NorBC complex). The values are given as the average ± standard deviation of measurements on *n* samples.

Polyacrylamide Gel Electrophoresis. SDS−PAGE was carried out in 13.5% acrylamide gels at 6 °C. Samples for electrophoresis were prepared by addition of an equal volume of a sample buffer containing 16% SDS without reductant and applied after a short incubation at room temperature.

Silver staining was carried out as described previously (*20*) to maximize sensitivity. Heme staining of gels was performed by incubation with tetramethyl-benzidine and development with hydrogen peroxide (*24*).

Activity Measurements. NO was produced chemically by the reaction of $NaNO_2$ with Cu in an acidic environment or purchased from Messer Griesheim (Frankfurt am Main, Germany). All solutions were degassed under vacuum, and the apparatus was flushed extensively with nitrogen gas prior to use. The NO gas was washed with 4 M NaOH to hydrolyze any N_2O present before bubbling through unbuffered water, which had been adjusted to pH 3 with HCl to prevent formation of NO_2^-. This stock solution was prepared in a septum-sealed glass vessel and only used on the day of preparation. At saturation, the NO concentration was assumed to be 1.9 mM at 20 °C. The reduction of NO was measured polarographically with an Au/Ag electrode, polarized at 0.8 V (*25*) at 30 °C. The standard reaction medium (1 mL) consisted of 50 mM Hepes-KOH, 50 mM KCl, and 0.02% DM, pH 7.1. The routinely used electron donors were *N*,*N*,*N*′,*N*′-tetramethyl-*p*-phenylenediamine (TMPD, 1.5 mM) and sodium ascorbate (5 mM). Anaerobic conditions were created via the glucose/glucose oxidase/catalase system (16 mM, 4 units/mL, 20−25 units/mL, respectively). Maximal slopes which are obtained at low NO concentration (*12*) were used for rate calculations.

Hydrodynamic Measurements. Analytical ultracentrifugation was performed with a Beckman XL-A Ultracentrifuge using an An50Ti rotor with a 0.3 cm double sector cell at 4 °C. Protein was monitored at 280 or 411 nm, and data were analyzed using the Ultrascan Analytical Ultracentrifugation Software (B. Demeler, University of Texas Health Science Center, Texas). The average sedimentation coefficient was determined at 30 000 rpm excluding the extreme 10% of the boundary. The molecular weight of protein (M_p) was calculated from the sedimentation equilibrium measurements at 5000 rpm, 4 °C, using the equation

$$\Delta \ln C/\Delta r^2 = M_p (1 - \phi'\rho)\omega^2/2RT$$

where $(1 - \phi'\rho) = (1 - \upsilon_p\rho) + \sigma_d(1 - \upsilon_d\rho)$.

C is the concentration of protein over the distance from the center of rotation (r), ω is the angular velocity, R is the gas constant, and T is the temperature. ϕ' is the apparent partial specific volume which breaks into two components—the contributions of protein (υ_p) and detergent (υ_d). σ_d is the amount of bound detergent (g/g) and r is the density of solution. Partial specific volume of NOR (0.732 g/mL) was calculated from the predicted protein sequences, and that of DM (0.824 g/mL) as reported in ref *26*. The binding of DM to the purified NOR complex was determined by gel filtration (see above) in a buffer containing ^{14}C-labeled DM as described in ref *26*.

Two-Dimensional Crystallization and Electron Microscopy. Two-dimensional crystallization of NOR was carried out by dialysis of detergent from a protein/lipid/detergent mixture using bent glass tubes with an internal diameter of 3 mm as described previously (*20*). A mixture of L-α-phosphatidyl choline containing dimyristoyl and egg phosphatidyl choline in a 1:1 ratio was added to NOR (0.5 mg/mL) to give a lipid/protein ratio of 0.28 (w/w). Octanoyl sucrose was added to the final concentration of 1.5% (w/v) in the total volume 75 μL. The sample was dialyzed against 100 mM Tris-HCl, pH 8.6, containing 2 mM sodium azide at 37 °C. The formation of crystalline arrays was monitored by electron microscopy and optical diffraction of negatively stained specimens. Aliquots (2 μL) of crystalline specimens were applied to glow-discharged continuous carbon grids and frozen after blotting as described previously (*27*). Low electron dose images of crystals were recorded with a Phillips CM200 FEG electron microscope operated at 200 kV. Images were processed as described previously (*27*).

FTIR Spectroscopy. The cytochrome *bo* of *Escherichia coli* was purified as described in ref *28*. The NOR and cytochrome *bo* samples were prepared by repeated dilution into 0.6 M sodium phosphate, pH 7.0, and 0.3% (w/v) decylmaltoside, followed by concentration using centrifuge concentrators. NOR solution (2 μL) was placed on the top of a CaF_2 window under a stream of carbon monoxide and reduced by addition of 0.5 μL of 0.5 M sodium dithionite. CO gassing was continued for 3 min, and the mixture was homogeneously distributed by means of another CaF_2 window. The assembled cuvette was mounted into a thermostated sample holder of a Bruker IFS88 FTIR spectrometer, purged with dried air. After equilibration at −39 °C, a dark spectrum was recorded with 4000 scans. The sample was then photolyzed with a 100 W halogen lamp (power set to 80 W) equipped with a Schott KG2 heat filter. Recording of the light spectrum (4000 scans) was started 1 min after the initiation of photolysis under continuous illumination. The infrared radiation transmitted by a 2600 cm^{-1} low-pass filter was measured by a mercury cadmium telluride detector at spectral resolution 4 cm^{-1}.

EPR Spectroscopy. The samples for EPR were prepared as follows: 240 μL of NOR (65 μM) was mixed with 120 μL of 0.75 M Tris-Cl, pH 8.0, containing 75 mM NaCl and 0.01% DM. The sample was transferred to an EPR tube equipped with a vacuum line fitting. The atmosphere in the tube was replaced with argon; the tube was agitated in order to equilibrate the gas and liquid phases. After a few vacuum-argon flush-agitation cycles, the sample was frozen in liquid nitrogen and the EPR spectrum of the oxidized enzyme was recorded. The sample was thawed, and 4 μL of 100 mM TMPD and 7 μL of 500 mM Tris-ascorbate, pH 7, were added under argon counterflow. The sample was incubated for 10 min on ice, after which it was frozen again for recording of the spectrum of the reduced sample. After this, the sample was again thawed. The gas manifold of the vacuum line was evacuated and filled with NO (from AGA, >99% pure). The NO gas was cryo-pumped to a glass trap cooled with liquid nitrogen. Finally, the cold trap was allowed to warm slightly and the distilled colorless NO gas was allowed to enter the EPR sample tube coupled to the vacuum line. The sample was mixed by agitation and frozen in liquid nitrogen within a few minutes.

EPR spectra were recorded with a Bruker ESP 300 X-band spectrometer equipped with an ESR-900 liquid helium cryostat manufactured by Oxford Instruments. Bruker ESP 1600 software version 2.2 was used in handling the spectra. Sample temperature was 12 K, modulation frequency 100 kHz, and microwave frequency 9.427 Ghz. Each spectrum is a sum of two scans.

Miscellaneous. N-terminal sequencing by Edman degradation of blotted protein subunits, and mass spectrometry

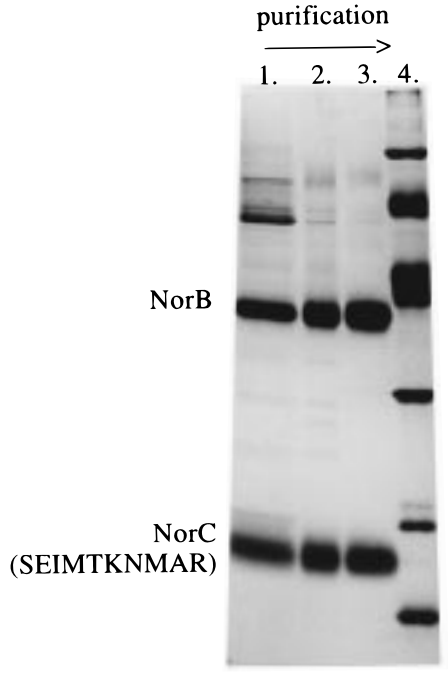

FIGURE 1: Polypeptide composition of the NOR preparations after the first QSHP column (lane 1), the IMAC column (lane 2), and the final preparation after the second QSHP column (lane 3). The NOR subunits are indicated on the left with the N-terminal sequence determined for NorC, and the molecular weight markers are in the lane 4.

of the solubilized complex and peptide digests were performed by the protein and peptide sequencing service at the EMBL, Heidelberg.

RESULTS AND DISCUSSION

Purification. We have developed a new purification procedure for NOR of *Pa. denitrificans*. The PD21.27-(Δcbb_3) strain was chosen as the starting material in order to facilitate the identification of the enzyme and to eliminate any possibility of contamination with the cbb_3-type cytochrome oxidase which is also a cytochrome *bc* complex (*18*). The purification protocol is based on anion exchange and metal-ion affinity chromatography. Purification was followed spectroscopically using the previously established characteristics (*29*) of the reduced *minus* oxidized visible spectrum and SDS−PAGE (Figure 1) as well as by NOR activity. The results of a typical purification procedure are outlined in Table 1.

The enzyme was solubilized using dodecyl maltoside and applied to a QSHP column. The fractions containing NOR eluted from this first column approximately at 0.4 M NaCl immediately after green fractions containing cytochrome aa_3. NOR subsequently bound as a tight band to the top of the IMAC column whereas most of the contaminating proteins were not bound at all or were eluted when the column was washed with 5% buffer B (see Materials and Methods). The subsequent purity of the NOR fraction depends on the extent of the washing step and on a complete return to baseline of the UV absorbance prior to the implementation of the second gradient. The bound NOR which was spread down the column by this stage, was eluted in a minimum volume using a steep imidazole gradient. After dilution, NOR bound tightly to the top of the second QSHP column and eluted at 0.4 M NaCl as a single peak. Further chromatography on a gel filtration column does not increase the purity of the enzyme which is 99% as based on the heme content and protein concentration determined as described in Materials and Methods. The typical yield is 15 mg of pure NOR from 1 g of membrane protein (Table 1). The purified NOR loses activity when stored under air. However, the activity is stable over two months at +4 °C if the enzyme is stored under nitrogen.

Table 1: Purification of the *Paracoccus denitrificans* NO Reductase[a]

	Protein (mg)	Heme B/C ratio	Purity (%)	Total activity (μmol/min)	Specific activity (μmol/min/mg)
membranes	595			1190	2.0
solubilized membranes	475			878	1.9
QSHP 1	22.5	2.05	61	526	23.4
IMAC	11	2.1	79	404	36.7
QSHP 2	9	2.1	99	353	38.4

[a] Protein quantitation was made by the BCA method for stages 1−3 and using the molar absorptivity at 280 nm for stages 4 and 5. Heme B/C ratios are given for the fractions containing only NOR. Purity is calculated from predicted protein concentration derived from heme content (B and C), divided by the determined protein concentration. Activities are the average of duplicate measurements.

Composition of the Purified Complex. The NOR complex is composed of two major polypeptides with apparent molecular weights of 38 and 17 kDa. Only trace amounts of other bands are detectable on silver-stained acrylamide gels (Figure 1). The presence of a 65 kDa band can be increased by heating the samples prior to electrophoresis; its intensity is reduced by running gels at 6 °C as previously found (*12*, *13*). This band probably corresponds to a dimeric form of NorB.

We identified the 17 kDa band as NorC by N-terminal sequencing. The sequence (SEIMTKNMAR) lacks the initial methionine residue. The 38 kDa band was found to have a blocked N-terminus. It was identified as NorB by mass spectrometry of peptides generated by a cleavage with cyanogen bromide. Four peptides with masses matching predicted CNBr-peptides of NorB were found, including the N-terminal peptide (amino acid residues 2−17; the sequence as reported in ref *5*).

The visible absorbance spectrum of the NOR preparation with an absorbance maximum at 550 nm with a shoulder at 560 nm in the reduced spectrum is consistent with the presence of both C- and B-type hemes and identical to those reported before (*12*, *15*, *17*, *29*). Heme staining of the electrophoresis gels (not shown) indicates that NorC contains covalently bound heme in accordance to the presence of an attachment motif for heme C in the sequence (*5*, *30*). Moreover, electrospray mass spectrometry showed that NorC has a molecular mass of 17 476 Da, which matches very well with the predicted weight of 17 477 Da for the mature protein (16 859 Da) with covalently bound heme C containing iron (618 Da).

Heme analysis by the pyridine hemochrome method indicates that the complex contains hemes B and C with a ratio of 2.1 ± 0.1 ($n = 6$). The metal analysis confirms the previous evidence for the absence of copper in the purified NOR samples [summarized by Zumft (*4*)]. The amount of

iron in the complex as assessed by flameless atomic absorption is 3.8 ± 0.3 Fe/NorBC complex ($n = 5$), while 0.8 ± 0.2 nonheam iron/complex is detected colorimetrically ($n = 5$). The measurements using TXRF resulted in the value 3.5 ± 0.2 Fe/complex ($n = 3$). Copper is not detected by flameless absorption and is below quantification by TXRF (<0.02). No other possible metal cofactors such as K, Cr, Mn, Co, Ni, or Zn can be identified by TXRF. However, Ca was invariantly detected in varying amounts (2.8 ± 1.6, $n = 3$).

Enzymic Activity. The NOR activity is nonlinear (*12*). The turnover rate increases toward the low NO concentration when the reaction is started by addition of the oxidized enzyme; the apparent K_m is about 2 mM. This phenomenon has been explained by binding of NO to the oxidized enzyme which causes substrate inhibition (see ref *12*). For our standard assay, the enzyme was always incubated in the presence of reducing agents prior to starting the reaction by addition of NO. Using the conditions of our standard assay at pH 7.1 (see Materials and Methods) with TMPD (1.5 mM) and ascorbate (5 mM) as electron donors, the maximal activity is ca. 40 mmol/mg/min (46 e^-/s). Nitrate and nitrous oxide do not affect the NOR activity, but nitrite at millimolar concentrations is a potent inhibitor (10 mM NO_2^- reduces activity to 50%).

Hydrodynamic Molecular Weight. The amount of detergent bound to the complex with an apparent molecular mass of 260 kDa as determined by gel filtration is 87 wt %. This implies that the complex is a dimer of two NorBC monomers in dodecyl maltoside under the given conditions (see Materials and Methods). The homogeneous character of the preparation was confirmed by native PAGE in the presence of Coomassie Blue (ref *31*; data not shown) and by analytical ultracentrifugation (Figure 2). Sedimentation velocity profiles show that NOR sediments as a single homogeneous species with an apparent sedimentation coefficient 9.8 S. The predicted molecular weight of the monomeric NorBC holoenzyme is 71.5 kDa. The analysis of sedimentation equilibrium data indicates that the molecular mass of the protein component is 150−160 kDa, again indicating that NOR is a dimer in the detergent complex (Figure 2).

Two-Dimensional Crystals. Two-dimensional crystals of the purified NOR were grown with phosphatidyl choline. The dialysis of octanoyl sucrose results in the formation of tubular structures which appear as flattened tubes in electron micrographs. These contain well-ordered crystalline arrays which can be used for processing of images produced by electron cryo-microscopy (Figure 3). The lattice (space group $P22_12_1$) shows that the enzyme is a dimer with the 2-fold symmetry axis perpendicular to the membrane. These images have thus far been processed at 8 Å resolution, and further analysis is needed for a proper comparison of NorBC with the cytochrome oxidase structures.

FTIR Spectroscopy. We compared the binding of carbon monoxide to the *E. coli* cytochrome *bo* quinol oxidase which is a heme/copper cytochrome oxidase, and to NOR, using FTIR spectroscopy. The spectroscopic differences between the light and dark states of the enzymes are displayed in Figure 4. The absorbance differences could only be observed under continuous light at −39 °C, which indicates full relaxation and reversibility of the ligand-exchange reaction at this temperature.

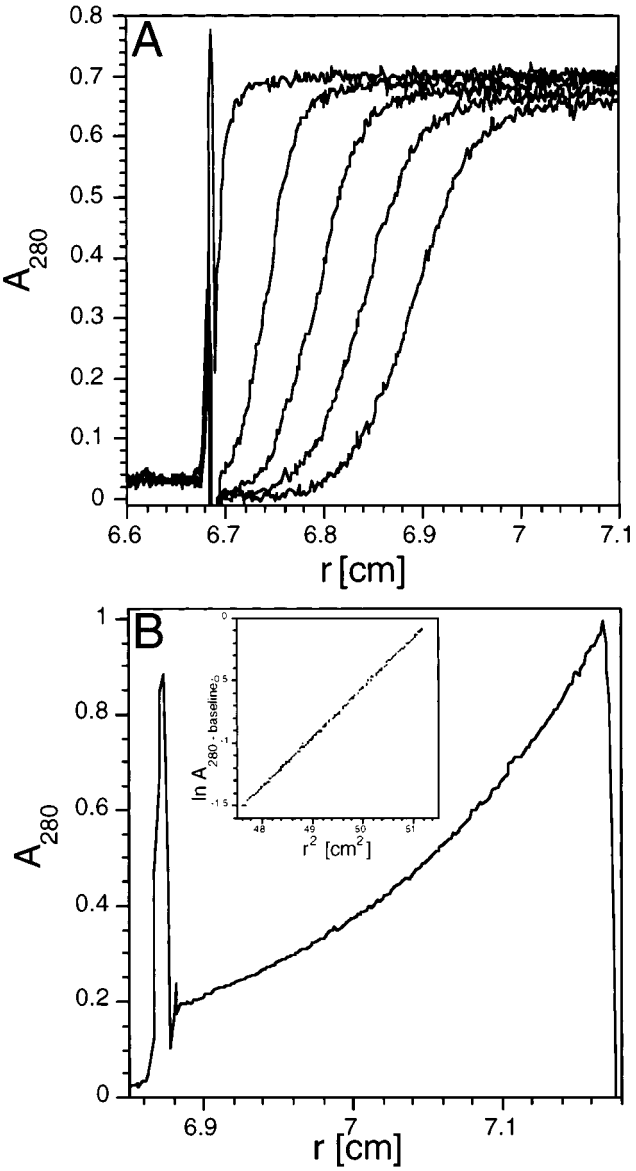

FIGURE 2: Analytical ultracentrifugation data from a sedimentation velocity (A) and a sedimentation equilibrium experiment (B). The rotor speed was 30 000 rpm (A) and 5000 rpm (B), and temperature 4 °C in both cases. The initial concentration of NOR was 10 μM in 20 mM Tris-HCl, pH 7.6, 125 mM NaCl, and 0.02% DM. Inset in B shows the analysis of the equilibrium data. The axis (r) is the distance from the center of rotation.

Free CO has a carbonyl stretching frequency of 2143 cm^{-1} (*32*), which could not be observed, because all ligand molecules are immobilized by the protein. In the dark, the negative deflections of difference spectra show that the stretching frequency of CO is lowered to 1959 and 1977 cm^{-1} upon binding to cytochrome *bo* and NOR, respectively. Optical spectroscopy has shown that the binding site of CO is the high-spin heme O of cytochrome *bo* and a heme B of NOR (*12*). During photolysis of the cytochrome *bo* complex, CO dissociates from heme O. The Cu_B center offers a second binding site to the dissociated ligand due to its closeness to the heme iron (Figure 4A). The Cu−CO complex has a carbonyl band at 2065 cm^{-1} which is reflected in a positive deflection of difference spectrum (*33*, *34*).

A different CO complex is formed when CO is photolyzed from the active-site heme B of NOR (Figure 4B). A

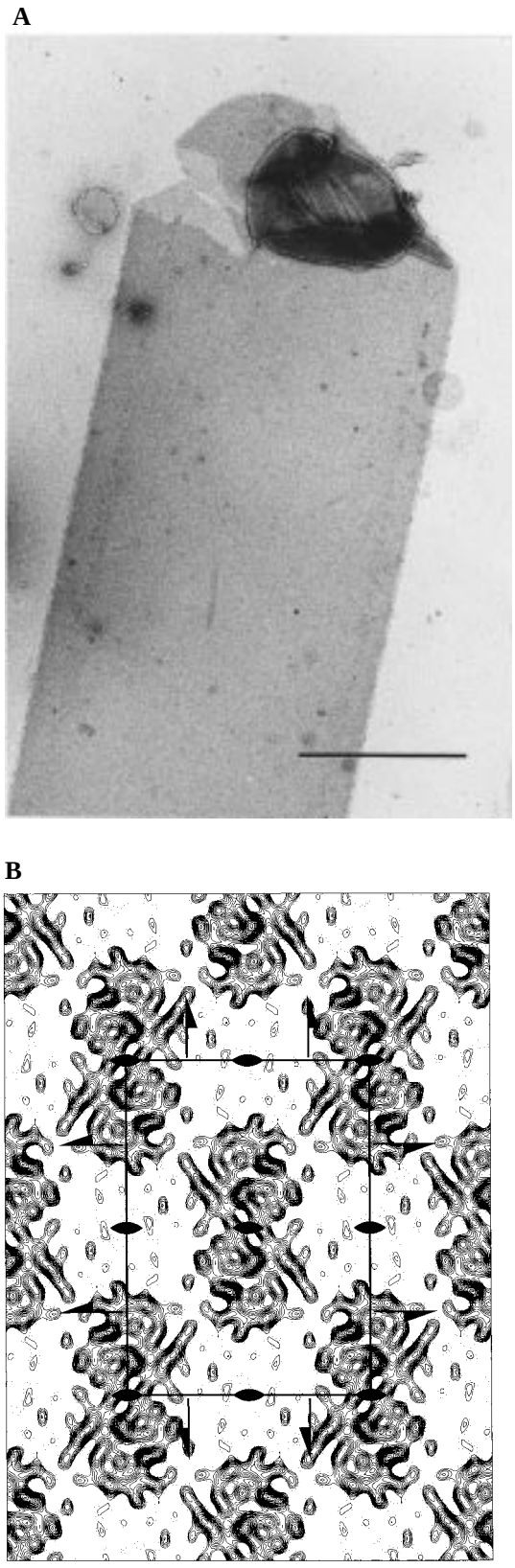

FIGURE 3: (A) A part of a tubular crystal of NOR. The crystal has been negatively stained with uranyl acetate. Scale bar represents 0.5 μm. (B) Projection map with $P22_12_1$ symmetry calculated from the amplitudes and phases of a single image after processing. One unit cell (a = 128.6 Å, b = 92.8 Å) is outlined with the a-axis vertical and b-axis horizontal. The map has been contoured in steps of 0.2 × rms density. Negative density [0.0 − (−0.4) s] is indicated by dotted line. Symmetry elements are marked. The dimer consists of two NorBC complexes that are related by a crystallographic 2-fold rotation axis perpendicular to the membrane.

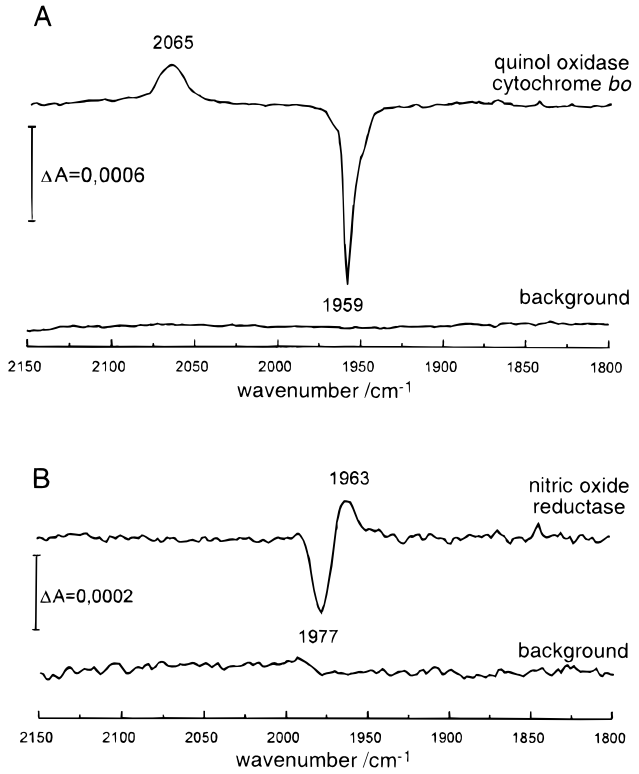

FIGURE 4: Absorbance difference FTIR-spectra of CO complexes before and after photolysis of the *E. coli* cytochrome *bo* (A) and the *Paracoccus* NOR (B). The spectra taken in the dark (downward deflections) were subtracted from the spectra taken in the light (upward deflections). The difference spectra are averages from six spectra each consisting of 4000 scans. Prior to photolysis, the background spectra were taken under identical conditions in the dark.

Table 2: Summary of FTIR Data

CO complex	wavenumber (cm^{-1})	$\Delta\nu_{1/2}$ (cm^{-1})
cytochrome *bo* (heme O)	1959	8
Cu_B	2065	20
NO reductase (heme B)	1977	11
non-heme Fe	1963	13

Cu−CO adduct cannot be responsible for the carbonyl signal at 1963 cm^{-1}, because there is no copper in NOR. In this case, the binding of dissociated CO has to be assigned to another metal located in the vicinity of the heme. The other heme in NorB is low spin (*17*), and in the light, even a transient binding to such metal center would be highly improbable. Therefore, we suggest that the association of CO with the nonheme iron is responsible for the positive absorption signal in NOR. In their apoprotein−liganded states, the outer shell electron density of Fe^{2+} is smaller than of Cu^+, allowing much less electron back-donation to the π-acceptor ligand CO (*32*). This would explain the difference in absorbance frequencies of 2065 cm^{-1} for Cu_B−CO and of 1963 cm^{-1} for the nonheme Fe−CO.

The bandwidth at the half-peak height ($\Delta\nu_{1/2}$) (Table 2) is much smaller for the heme-carbonyl band of cytochrome *bo* than that of NOR, suggesting higher polarity in the latter heme pocket. In contrast, the absorbance band of the proposed nonheme Fe−CO is narrower than the band of Cu_B−CO. This may suggest that the catalytic center of NOR is more homogeneous with respect to its overall polarity than that of the heme/copper oxidases.

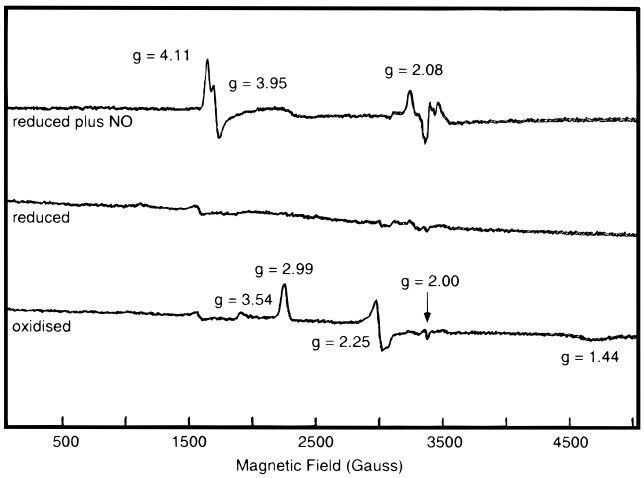

FIGURE 5: EPR spectra of the *Paracoccus* NOR. EPR spectra of 43 μM NOR, recorded sequentially from a sample made as described in Materials and Methods. Note the differences in the signals at $g = 4$ (nonheme iron) and $g = 2$ (nitrosyl-ferroheme) in the spectrum recorded after introduction of NO to the reduced sample (the uppermost spectra). This spectrum was obtained by thorough mixing of the sample with NO from the gas phase prior to freezing. Microwave power, 2.0 mW; modulation amplitude 19.8 G; scanning speed, 29.8 G/s.

EPR Spectroscopy. Our enzyme preparation appears to be free of contaminating iron proteins, which may give rise to additional EPR signals in many NOR preparations. The spectrum of the oxidized enzyme shows two low-spin heme signals. One has a set of *g*-values at 2.99, 2.25, and 1.44, whereas only one resonance at $g = 3.54$ is observed for the other (Figure 5). These signals can be assigned to the cytochrome *c* and the low-spin cytochrome *b* components of NOR (*16*, *17*). Practically no signals are seen at $g = 6$ or $g = 2$ in the oxidized NOR. In contrast to the spectrum reported in ref *12*, there is no signal at $g = 2.009$. In essence, only two low-spin hemes are seen, which suggests that the high-spin heme is magnetically coupled to another paramagnet (see also ref *17*).

Both low spin signals disappear, as expected, upon reduction of NOR. When NO is added to the reduced enzyme and the sample is mixed thoroughly before freezing, two strong signals appear at $g = 4$ and 2 (Figure 5). The latter is probably a mixture of two signals. The appearance of these signals reflects the breakage of magnetic coupling between the ferrous high spin heme and a ferrous (high spin) nonheme iron when both irons form complexes with NO. The complex resonance at $g = 2$ with a peak at $g = 2.08$ resembles those observed with a number of nitric oxide complexes of other heme proteins (*35*, *36*) and is caused by a typical nitrosyl-ferroheme.

The signal at $g = 4$ with components at $g = 4.11$, 3.95, and 2.0 is of particular interest (Figure 5). It most likely arises from a $S = {}^3/_2$ FeNO system in which a high spin ferric ($S = {}^5/_2$) nonheme iron is antiferromagnetically coupled to NO^- ($S = 1$) (*37*−*41*). We suggest that the $g = 4$ signal is brought about by an Fe(II)−NO complex with $S = {}^3/_2$ and indicates the presence of a nonheme iron in the active site of NOR.

The EPR data show that there are two ferrous irons in the active site and both are able to bind NO under turnover conditions, behaving like independent mononuclear centers in the ligand binding. It may be relevant for the catalytic activity of NOR that the bound NO acquires the character of nitroxyl anion NO^- (cf. ref *41*). The dimerization of two such anions (the other is generated at the heme) with subsequent protonation reactions and cleavage of water would yield N_2O (cf. refs *3*, *12*, and *14*). This reaction is very fast even when it is not catalyzed by an enzyme, and it is an attractive mechanism for NO reduction. It is possible that only nitroxyl anion can dissociate from the ferrous heme during catalysis (although the low midpoint potential of this reaction has been suggested to pose a problem, cf. refs *1* and *2*), so that NO is effectively trapped by the heme after consumption of the reductant. This could mean that the binuclear iron center is unlikely to become fully oxidized during the normal catalytic cycle in the absence of oxygen.

CONCLUSIONS

Structure of the Bacterial NOR. The analysis of the *nor* gene loci has suggested that the enzyme may contain more than two subunits (NorB and NorC) in situ (*2*, *5*, *8*). In particular, one of the open reading frames encodes a protein that is homologous to subunit III of the heme-copper oxidases. Using dodecyl maltoside, a mild detergent which facilitated the first isolation of three- and four-subunit preparations of cytochrome aa_3 oxidase from *Paracoccus* (*42*, *43*), we anticipated that a NOR complex will purify with additional subunits. However, there is no evidence for more than two polypeptides in the purified complex under any conditions employed in the protocol. We may thus conclude that the two-subunit complex appears to carry the full enzymatic activity (Table 1) even if additional protein components associate with the NorBC complex in the cytoplasmic membrane.

The NorBC complex is a dimer both in membranes and in detergent solution. There is, however, no indication that this bears any relevance for the catalytic function. The complex kinetics can be explained by the inhibitory effect of NO which binds to the oxidized enzyme blocking the turnover (*12*).

The Dinuclear Fe−*Fe Active Site.* Metal analysis and spectroscopic data indicate that the active site in NorB is a dinuclear iron center made of a heme and a nonheme iron. The homology to COX1 suggests that the three histidine ligands of Cu_B in transmembrane helices coordinate to the nonheme iron in NorB (*8*, *9*). However, unlike copper, the nonheme iron is expected to have up to six ligands. Our data show that at least one of the ligand positions is available for NO, leaving two ligands unknown. The EPR spectrum of the $S = {}^3/_2$ iron-NO complex is similar to that of soybean lipoxygenase in the presence of ethanol (*38*). In the structure of the lipoxygenase (*44*, *45*), the iron is strongly ligated by three imidazoles and a carboxylate oxygen; the additional ligands are a weakly bound asparagine and a water molecule. The inspection of aligned NorB and COX1 sequences shows that there are conserved glutamates specific for the NORs. One in the predicted trans-membrane helix VI and the other in helix VIII could be within bond-forming distance from the nonheme iron (*8*). A modeling exercise (*9*) has not been able to introduce a role in direct metal coordination for these carboxylates. The determination of a high-resolution experimental structure is required for understanding of the coordination around the nonheme iron.

This paper and the recent MCD and EPR data on the oxidized NOR of *Ps. stutzeri* (*17*) firmly establish the chemical nature of the active site in NOR and confirm the prediction made by sequence homology that this enzyme is similar to the heme-copper oxidases. The structural variations between the heme-iron nitric oxide reductase and the heme-copper cytochrome oxidases must in part reflect the chemical difference of the respective catalytic reaction. They will be subject to future studies.

ACKNOWLEDGMENT

We are grateful to Rob van Spanning (Vrije Universiteit Amsterdam) for supplying the PD21.27(Δcbb$_3$) strain and to Marc le Maire (Gif-sur-Yvette, France) for his donation of ^{14}C-labeled dodecyl maltoside. We also thank Myles Cheesman (Norwich, England) for communicating data prior to publication, as well as Joel Morgan (Helsinki, Finland) and Axel Wittershagen (Frankfurt, Germany) for expert help with the vacuum line and metal analysis, respectively.

REFERENCES

1. Averill, B. A. (1996) *Chem. Rev. 96*, 2951−2964.
2. Zumft, W. G. (1997) *Microbiol. Mol. Biol. Rev. 61*, 533−616.
3. Berks, B. C., Ferguson, S. J., Moir, J. W. B., and Richardson, D. J. (1995*) Biochim. Biophys. Acta 1232*, 97−173.
4. Zumft, W. G. (1993) *Arch. Microbiol. 160*, 253−264.
5. De Boer, A. P. N., van der Oost, J., Reijnders, W. N. M., Westerhoff, H. V., Stouthamer, A. H., and van Spanning, J. M. (1996) *Eur. J. Biochem. 242*, 592−600.
6. Saraste, M., and Castresana, J. (1994) *FEBS Lett. 341*, 1−4.
7. Van der Oost, J., de Boer, A. P. N., de Gier, J.-W., Zumft, W. G., Stouthamer, A. H., and van Spanning, R. J. M. (1994) *FEMS Microbiol. Lett. 121*, 1−10.
8. Hendriks, J., Gohlke, U., and Saraste, M. (1998*) J. Bioenerg. Biomembr. 30*, 15−24.
9. Kannt, A., Michel, H., Cheesman, M. R., Thomson, A. J., Dreusch, A. B., Körner, H., and Zumft, W. G. (1998) in *NATO ASI Book Series* (Canters, G. W., and Vijgenboom, E., Eds.) Kluwer Academic Press (in press).
10. Iwata, S., Ostermeier, C., Ludwig, B., and Michel, H. (1995) *Nature 376*, 660−669.
11. Tsukihara, T., Aoyama, H., Yamashita, E., Tomizaki, T., Yamaguchi, H., Shinzawa-Itoh, K., Nakashima, R., Yaono, R., and Yoshikawa, S. (1995) *Science 269*, 1069−1074.
12. Girsch, P., and de Vries, S. (1997) *Biochim. Biophys. Acta 1318*, 202−216.
13. Heiss, B., Frunzke, K., and Zumft, W. G. (1989) *J. Bacteriol. 171*, 3288−3297.
14. Dermastia, M., Turk., T., and Hollocher, T. C. (1991) *J. Biol. Chem. 266*, 10899−10905.
15. Fujiwara, T., and Fukumori, Y. (1996) *J. Bacteriol. 178*, 1866−1871.
16. Sakurai, N., and Sakurai, T. (1997) *Biochemistry 36*, 13809−13815.
17. Cheesman, M. R., Zumft, W. G., and Thomson, A. J. (1998) *Biochemistry 37*, 3994−4000.
18. De Gier, J.-W. L., Schepper, M., Reijnders, W. N. M., van Dyck, S. J., Slotboom, D. J., Warne, A., Saraste, M., Krab, K., Finel, F., Stouthammer, A. H., van Spanning, R. J. M., and van der Oost, J. (1996) *Mol. Microbiol. 20*, 1247−1260.
19. Van Spanning, R. J. M., Wansell, C. W., Reijnders, W. N. M., Oltmann, L. F., and Stouthammer, A. H. (1991) *J. Bacteriol. 173*, 6962−6970.
20. Warne, A., Wang, D. N., and Saraste, M. (1995) *Eur. J. Biochem. 234*, 443−451.
21. Gill, S. C., and von Hippel, P. H. (1989) *Anal. Biochem. 182*, 319−326.
22. Berry, E. A., and Trumpower, B. L. (1987) *Anal. Biochem. 161* 1−15.
23. Wittershagen, A., Rostam-Khani, P., Klimmek, O., Grosse, R., Zickermann, V., Zickermann, I., Gemeinhardt, S., Kröger, A., Ludwig, B., Kolbesen, B. O. (1997) *Spectrochim. Acta B 52*, 1033−1038.
24. Thomas, P. E., Ryan, D., and Levin, W. (1976) *Anal. Biochem. 75*, 168−1176.
25. Carr, G. J., Page, M. D., and Ferguson, S. J. (1989) *Eur. J. Biochem. 179*, 683−692.
26. Møller, J. V., and le Maire, M. (1993) *J. Biol. Chem. 268* 18659−18672.
27. Gohlke, U., Warne, A., and Saraste, M. (1997) *EMBO J. 16*, 1181−1188.
28. Lübben, M., and Gerwert, K. (1996) *FEBS Lett*. 397, 303−307.
29. Carr, G. J., and Ferguson, S. J. (1990) *Biochem. J. 269* 423−429.
30. Zumft, W. G., Braun, C., and H. Cuypers (1994) *Eur. J. Biochem. 219*, 481−490.
31. Schägger, H. (1994) in *A Practical Guide to Membrane Protein Purification* (Schägger, H., and von Jagow, G., Eds.) pp 82−104, Academic Press, London.
32. Cotton, F. A., Wilkinson, G., and Gaus, P. L. (1987) *Basic Inorganic Chemistry*, J. Wiley & Sons, London.
33. Hosler, J. P., Ferguson-Miller, S., Calhoun, M. W., Thomas, J. W., Hill, J., Lemieux, L., Ma, J., Georgiou, C., Fetter, J., Shapleigh, J., Tecklenburg, M. M. J., Babcock, G. T., and Gennis, R. B. (1993) *J. Bioenerg. Biomembr. 25*, 121−136.
34. Garcia-Horsman, J. A., Berry, E., Shapleigh, J. P., Alben, J. O., and Gennis, R. B. (1994) *Biochemistry 33*, 3113−3119.
35. Yonetani, T, Yamamoto, H., Erman, J. E., Leigh, J. S., Jr., and Reed, G. H. (1972*) J. Biol. Chem. 247*, 2447−2455.
36. Morse, R. H., and Chan, S. I. (1980). *J. Biol. Chem. 255*, 7876−7882.
37. Rich, P. R., Salerno, J. C., Leigh, J. S., and Bonner, W. D., Jr. (1978) *FEBS Lett. 93*, 323−326.
38. Nelson, M. J. (1987) *J. Biol. Chem. 262*, 12137−12142.
39. Chen, V. J., Orville, A. M., Harpel, M. R., Frolik, C. A., Surerus, K., Munck, E., and Lipscomb, J. D. (1989) *J. Biol. Chem. 264*, 21677−21681.
40. Le Brun, N. E., Andrews, S. C., Moore, G. R., and Thomson, A. J. (1997) *Biochem. J*. 326, 173−179.
41. Zhang, Y., Pavlovsky, M. A., Brown, C. A., Westre, T. E., Hedman, B., Hodgson, K. O., and Solomon, E. I. (1992) *J. Am. Chem. Soc. 114*, 9189−9191.
42. Haltia, T., Puustinen, A., and Finel, M. (1988) *Eur. J. Biochem. 172*, 543−546.
43. Haltia, T., Semo, N., Arrondo, J. L. R., Goni, F. M., and Freire, E. (1994) *Biochemistry 33*, 9731−9740.
44. Boyington, J. C., Gaffney, B. J., and Amzel, L. M. (1993) *Science 260*, 1482−1486.
45. Minor, W., Steczko, J., Stec, B., Otwinowski, Z., Bolin, J. T., Walter, R., and Axelrod, B. (1996) *Biochemistry 35*, 10687−10701.

BI980943X